2019 SECED Conference
Earthquake risk and engineering towards a resilient world
9-10 September 2019, Greenwich, London

SIMULATING THE DYNAMIC PERFORMANCE OF TYPICAL URM CAVITY-WALL SYSTEMS BY THE APPLIED ELEMENT METHOD

Daniele MALOMO[1], Rui PINHO[2,3] & Andrea PENNA[4]

Abstract: *The terraced house building typology, which typically consists of low-rise unreinforced masonry (URM) constructions with cavity-walls, rigid floor diaphragms and timber roof, is largely widespread in a number of countries exposed to tectonic or induced seismicity. Experimental evidence has shown that the lack of seismic details, as well as the presence of large openings at the ground floor, makes these structures particularly vulnerable towards horizontal actions. Their assessment, given the large variability of construction techniques and masonry properties from one region to another, may benefit significantly from validated numerical models able to predict the global dynamic behaviour until up to complete collapse. In this paper, advanced discontinuum-based models developed within the framework of the Applied Element Method, are employed for replicating the shake-table response of a series of full-scale building prototype representative of cavity-wall terraced houses construction, tested up to collapse or near collapse conditions. A novel methodology for accounting explicitly for the influence of the presence of both rigid and flexible diaphragms, degree of connections among structural members and interaction between in-plane and out-of-plane mechanisms, is proposed. The introduction of specific simplified assumptions and empirical expressions, initially selected depending on the considered test and then extended to the general case, provided an acceptable representation of crack patterns, failure modes and hysteretic behaviours within a reasonable timeframe.*

Introduction

Unreinforced masonry (URM) terraced house construction typically comes in the form of low-rise residential buildings characterized by large openings at the ground floor, timber roof and cavity-walls, constituted by the assembly of a loadbearing inner leaf plus an outer veneer with only aesthetic and insulation functions. In some of the countries where this building typology is common (e.g. New Zealand, Australia, India), and in particular in the Central and Northern European region, the inner wall is often made of calcium silicate (CS) bricks, whilst the external leaf is constructed using clay (CL) masonry instead. As part of a wider experimental campaign (Graziotti et al. 2018) aimed at supporting the assessment of the seismic vulnerability of URM buildings in the Groningen region (The Netherlands), recently exposed to low-intensity ground motions due to gas extraction (van Elk et al. 2019), a number of full-scale specimens were tested on the shake-tables of both EUCENTRE (Pavia, Italy) and LNEC (Lisbon, Portugal) laboratories, including a two-story terraced house building specimen (i.e. EUC-BUILD1, Graziotti et al. 2017) and its 2nd story-roof (i.e. LNEC-BUILD1, Tomassetti et al. 2018) and attic-roof (i.e. LNEC-BUILD2, Correia et al. 2018) structural sub-assemblies. In the latter case, and after the attainment of the collapse of the gable walls, the timber roof was also subjected to a supplementary quasi-static cyclic pushover test for a complete characterisation of the diaphragm response.

Detailed numerical simulations of the dynamic response up to collapse of cavity-wall terraced house building typologies are needed for the development of seismic risk models in regions where these structures are present (e.g. Crowley et al. 2018). However, they were not readily available in the literature, most likely because their validation required shake-table tests on complete structural systems that only now have become available, through the experimental campaign cited above. Moreover, although recent applications have shown good agreement with shake-table test outcomes until up to near-collapse conditions (e.g. Chácara et al. 2018; Kallioras et al. 2019), simulating the complete collapse of complex URM systems still represents an open challenge. Indeed, while the use of simplified methods may lead to inaccurate results, given that

[1] Dr., University of Pavia, Pavia, Italy
[2] Professor, University of Pavia, Pavia, Italy
[3] Director, Mosayk Ltd, Pavia, Italy
[4] Professor, University of Pavia, Pavia, Italy

out-of-plane (OOP) failure modes are typically neglected, the employment of the majority of the presently-available advanced modelling strategies (e.g. FEM, DEM) might provide conservative results (as pointed out in e.g. Grunwald et al. 2018), often implying a prohibitive computational expense (see e.g. Galvez et al. 2018) or requiring the use of elaborated modelling strategies (e.g. Malomo et al. 2019).

In this work, the Applied Element Method (AEM), a rigid body and spring model originally conceived by Meguro and Tagel-Din (2000, 2001, 2002) for reproducing controlled demolition processes and collapse events of reinforced concrete large-scale structures (e.g. Calvi et al. 2018; Salem et al. 2014), and only recently applied to the modelling of complex URM assemblies (e.g. Karbassi and Nollet 2013; Malomo et al. 2018b), has been selected and employed for reproducing numerically the dynamic performance of the abovementioned URM full-scale specimens (i.e. EUC-BUILD1, LNEC1-BUILD1 and LNEC-BUILD2), up until to both near-collapse and collapse conditions. The different test specimens were modelled after the experimental campaign had been completed, and in opposite order with respect to the actual testing sequence, thus enabling the optimisation of the calibration process, and also allowing one to evaluate numerically the influence of several modelling assumptions, including the idealisation of nailed/screwed connections and tie elements in cavity-walls.

The AEM for masonry structures

Within the framework of AEM modelling of URM structures, an arbitrary masonry segment is composed of brick elements connected to each other by equivalent springs, in which the mechanical properties of brick-mortar interfaces are lumped, as depicted in Figure 1(a). A given brick can be modelled as a rigid block or as an assembly of units (if it is desired to model potential splitting or crushing of bricks, then the latter need necessarily to be discretised).

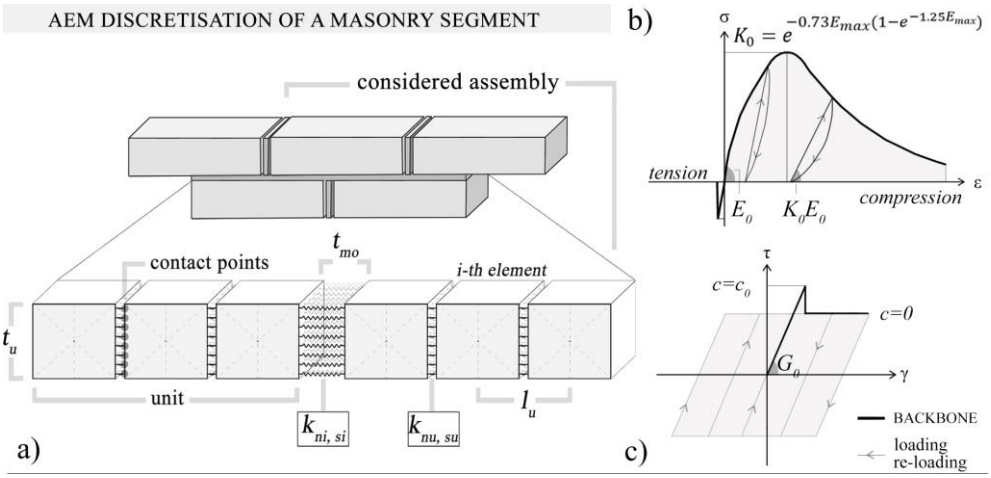

Figure 1 Three-dimensional discretisation of a masonry segment according to the AEM (a), interface springs constitutive laws under normal (b) and shear (c) cyclic loading

From a computational viewpoint, two different stiffness matrices are needed here: for the brick elements assembly, since the springs connect elements of identical material, $[K_{bg}]$ is composed of the brick stiffnesses k_{nu} and k_{su} only (Equation 1), whereas for the interfaces, $[K_{ig}]$ is made up inferring the equivalent stiffnesses k_{ni} and k_{si} (see Equation 2), obtained assuming the brick and mortar springs arranged in series at an arbitrary contact point).

$$k_{nu} = \sum_{i=1}^{j}\left(\frac{E_u\, d\, \left(\frac{t_u}{j}\right)}{l_e}\right), k_{su} = \sum_{i=1}^{j}\left(\frac{G_u\, d\, \left(\frac{t_u}{j}\right)}{l_e}\right) \quad (1)$$

$$k_{ni} = \sum_{i=1}^{j}\left(\frac{l_u - t_{mo}}{E_u\, d\, \left(\frac{t_u}{j}\right)} + \frac{t_{mo}}{E_{mo}\, d\, \left(\frac{t_u}{j}\right)}\right)^{-1},\ k_{si} = \sum_{i=1}^{j}\left(\frac{l_u - t_{mo}}{G_u\, d\, \left(\frac{t_b}{j}\right)} + \frac{t_{mo}}{G_{mo}\, d\, \left(\frac{t_u}{j}\right)}\right)^{-1} \quad (2)$$

The above parameters, representing the brick-mortar interaction, take into account both the brick and the mortar elastic properties. Naturally, in a post-cracked response stage, the elastic parameters implemented are modified according to the considered material constitutive laws. In the current version of the AEM-based commercial software employed in this endeavour, i.e. Extreme Loading for Structures (ASI 2018), as shown in Figure 1(b), a tension cut-off criterion (with no softening branch) is assigned to normal springs, as well as a simplified version of the elasto-plastic fracture model (EPF), originally developed by El-Kashif and Maekawa (2004), for simulating the cyclic cumulative damage of masonry elements subjected to uniaxial compression. A Mohr-Coulomb model (Figure 1(c)), instead, is typically employed for representing shear-compression modes at the joint level.

To faithfully represent damage mechanisms at the joint level, it is clear that each component of a given masonry element needs to be described in terms of its material properties. However, experimental campaigns rarely involve tests that would allow one to obtain all necessary material characterisation for units and mortar separately. Thus, undertaking the approach proposed in Malomo et al. (2018c), a number of formulae inferred through empirical (i.e. Jäger et al. 2004; Kaushik et al. 2007) and theoretical (i.e. Brooks and Baker 1998; Ciesielski 1999; Matysek and Janowski 1996; U.B.C. 1991) investigations were used to obtain first estimates of Young's and shear moduli of both mortar (E_{mo}, G_{mo}) and units (E_b, G_b), where direct experimental values were not available. Then, the ensuing average is considered for modelling purposes and the associated shear moduli are obtained assuming material isotropy. These values will be given in the next sections, together with the experimental ones.

Idealisation of construction details and modelling of flexible diaphragms

Typical Dutch cavity wall terraced house systems usually consists of low-rise residential units with rigid diaphragms (i.e. reinforced concrete (RC) slabs) at first and second floors, plus a timber roof. The RC slabs are only supported by the CS inner leaf transversal walls (it is recalled that the CL masonry veneer has no loadbearing function). Indeed, the gaps between the underneath of both 1st and 2nd floor RC slabs and the top edge of the non-bearing CS longitudinal façades are filled with mortar only after construction completion. Thus, their frictional resistance is likely to be limited due to lack of vertical compression, whilst the compressive strength was also likely affected by shrinkage phenomena; these two aspects have been accounted numerically by assigning reduced flexural and shear stiffness values to the corresponding interface springs. To avoid the explicitly modelling of pull-in and pull-out phenomena of tie-elements connecting CS and CL leaves (which would have implied a very high computational burden), and since they typically failed within the CL mortar bonds, a bilinear constitutive law with post-peak softening branch and tension cut-off (experimentally-determined through quasi-static pull-out tests by Messali et al. (2016)) was assigned to the CL wall-tie interfaces. On the CS panel side, instead, a linear elastic connection, characterised by the same flexural stiffness of the CS mortar, was employed.

Similarly, while the design of the RC slabs has been faithfully reproduced numerically, a simplified modelling strategy was undertaken for simulating the response of the flexible timber roofs, which in the case of all the tested specimens were constituted by one ridge beam, two 1.20m-spaced joists per side among the ridge beam and two timber plates rigidly connected to RC foundation. Timber planks (182x18 mm), covered by ceramic tiles, were placed on top using a couple of 60x2 mm steel nails. In this framework, the contribution of nailed connections is accounted by a zero-thickness interface joint characterized by a rotational stiffness k_{φ}, while both joists and planks were modelled as solid elements with linear elastic behaviour (Gattesco and Macorini, 2014). Finally, both flexural and shear deformability contribution of timber boards to the in-plane response of the diaphragm were considered by defining an equivalent shear modulus for plank elements, as suggested by Brignola et al. (2012). Interested readers may refer to e.g. Malomo (2019) for the complete set of parameters employed for the modelling of the roof.

With a view to assess the effectiveness of the abovementioned simplified strategies, and after a comprehensive validation process that comprises the modelling of several URM components subjected to both in-plane (Malomo et al. 2018c) and OOP (Malomo et al. 2018a) loading, the in-plane quasi-static response of a full-scale timber sub-structure, tested by Correia et al. (2018) and representative of a typical pitched roof system used in the terraced houses object of the experimental campaign considered in this study, was reproduced numerically. Such experiment followed the shake-table test on the complete specimen (i.e. LNEC-BUILD2), where the URM gable walls collapsed in an OOP fashion, as shown in the subsequent section, and it was

performed after restoring the original configuration of the roof system. Two quasi-static full cycles of horizontal displacement were imposed to the ridge beam through steel ties fixed to the lab strong walls, at ±10, ±50, ±100 and ±150mm. As can be observed from Figure 2, a comparable response was obtained numerically, with the model producing acceptable results both in terms of deformed shape and hysteretic curve, albeit the capacity was slightly overestimated in the last cycles. Similarly, the evolution of displacements between the different roof joists (i.e. J1-J5), which remained linearly proportional to their elevation during the test, was adequately captured. Giving the encouraging results obtained, the same strategy was also employed for the modelling of the building-scale models presented in the subsequent sections.

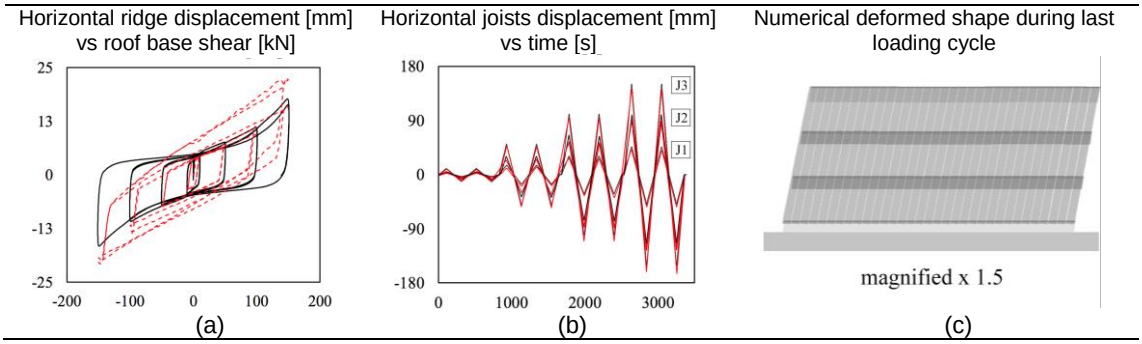

Figure 2. Exp. (black line) vs num. (red dashed line): (a) hysteretic response of the diaphragm, (b) relative displacement among timber joists J1-2-3 and (c) numerical deformed shape

Simulation of shake-table tests on URM building sub-structures

The LNEC-BUILD2 prototype was a full-scale timber roof with ceramic tiles, supported on URM gables constituted by cavity-walls (2 ties/m^2) on an RC slab, representative of the attic-roof system of EUC-BUILD1. Thus, the seismic input introduced at the base of LNEC-BUILD2 specimen corresponded to the second floor accelerations that had been recorded during the EUC-BUILD1 test. It was 5.82m long, 5.46m wide and 2.45m high with a total mass of 17.8 tons. With reference to the nomenclature reported in Figure 3(a) it is noted that the CL veneer was not present on the East side, because the specimen was meant to represent the end-unit of a set of terraced houses. Further details can be found in Correia et al. (2018). The LNEC-BUILD1 building specimen (see Figure 3(b)), instead, was meant to represent the upper levels of the EUC-BUILD1 specimen. It consisted of a single-story full-scale prototype 5.82 m long, 5.46 m wide and 4.93 m high with a total mass of 31.7 tons, with cavity-walls (2 ties/m^2) and pitched timber roof covered by ceramic tiles. The gable-diaphragm system was substantially analogous to LNEC-BUILD2 in terms of both construction details and overall geometry.

Figure 3. Plan (in cm) and experimental configuration of both (a) LNEC-BUILD2 (Correia et al. 2018) *and (b) LNEC-BUILD1* (Tomassetti et al. 2018)

The LNEC-BUILD2 and LNEC-BUILD1 specimens, both tested at LNEC laboratory, were subjected to incremental uniaxial (longitudinal E-W direction) and biaxial (longitudinal E-W and vertical direction) dynamic loading respectively, up to collapse. Full details on the imposed acceleration time-histories can be found in Correia et al. (2018) and Tomassetti et al. (2018). Both experimental and derived material properties, including compressive strength of masonry fc_m, flexural bond strength f_w, cohesion c and friction coefficient μ, have been directly implemented in the models, as reported in Table 1:

Table 1 Experimental and inferred material properties of LNEC-BUILD2 and LNEC-BUILD1

		CS - density δ_m = 1796 [kg/m^3]								CL - density δ_m = 1833 [kg/m^3]							
LNEC-BUILD2		fc_m	fc_b	f_w	E_m	c	μ	E_b	E_{mo}	fc_m	fc_b	f_w	E_m	c	μ	E_b	E_{mo}
	Avg [MPa]	7.0	18.7	0.3	6090	0.4	0.5	8990	2662	16.2	63.2	0.2	12661	0.4	0.7	7211	3535
	C.o.V. [%]	0.1	0.1	0.2	-	-	-	0.4	-	0.l	0.1	0.5	-	-	-	0.2	-
		CS - density δ_m = 1800 [kg/m^3]								CL - density δ_m = 1839 [kg/m^3]							
LNEC-BUILD1		fc_m	fc_b	f_w	E_m	c	μ	E_b	E_{mo}	fc_m	fc_b	f_w	E_m	c	μ	E_b	E_{mo}
	Avg [MPa]	9.8	16.3	0.4	7955	0.4	0.5	8990	4537	19.4	32.5	0.2	13118	0.4	0.8	7211	3332
	C.o.V. [%]	0.1	0.1	0.2	0.2	-	-	0.4	-	0.l	0.1	0.5	0.1	-	-	0.2	-

For what concerns LNEC-BUILD2, a comparison between numerical and experimental hysteretic behaviour for selected test cycles and final crack pattern is proposed in Figure 4, from which it can be gathered that the predicted force-displacement response marginally underestimated both energy dissipation and deformation capacity in the first cycles, although a seemingly acceptable agreement with experimental results in terms of initial and residual stiffness, base shear and overall resistance could be found.

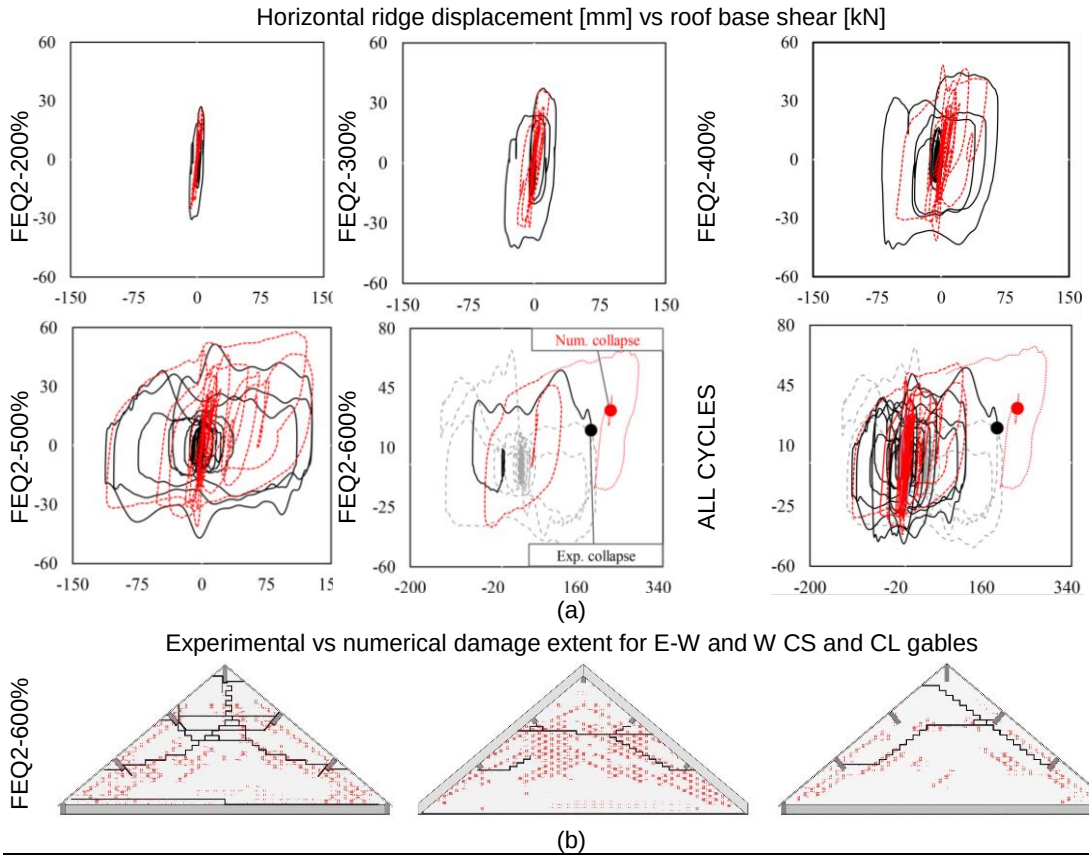

Figure 4. LNEC-BUILD2: Exp. (black line) vs num. (red dashed line) hysteretic response and crack pattern

Similarly, the response predicted in the case of LNEC-BUILD1 appears in good agreement with the one exhibited by the specimen (see Figure 5a), both in terms of overall capacity and displacement demand, though the energy dissipation was not always fully captured; this latter aspect might be due to the simplified tension cut-off criterion implemented in the interface springs, which in case of flexural damage neglects the post-peak energy dissipation. Numerical collapse occurred slightly before the actual experimental one, which may explain the differences in the hysteresis curves of FEQ2-300%. However, the damage evolution, as well as the OOP failure mechanism of the CS single leaf wall, was captured in a relatively satisfactory manner, as depicted in Figure 5(b).

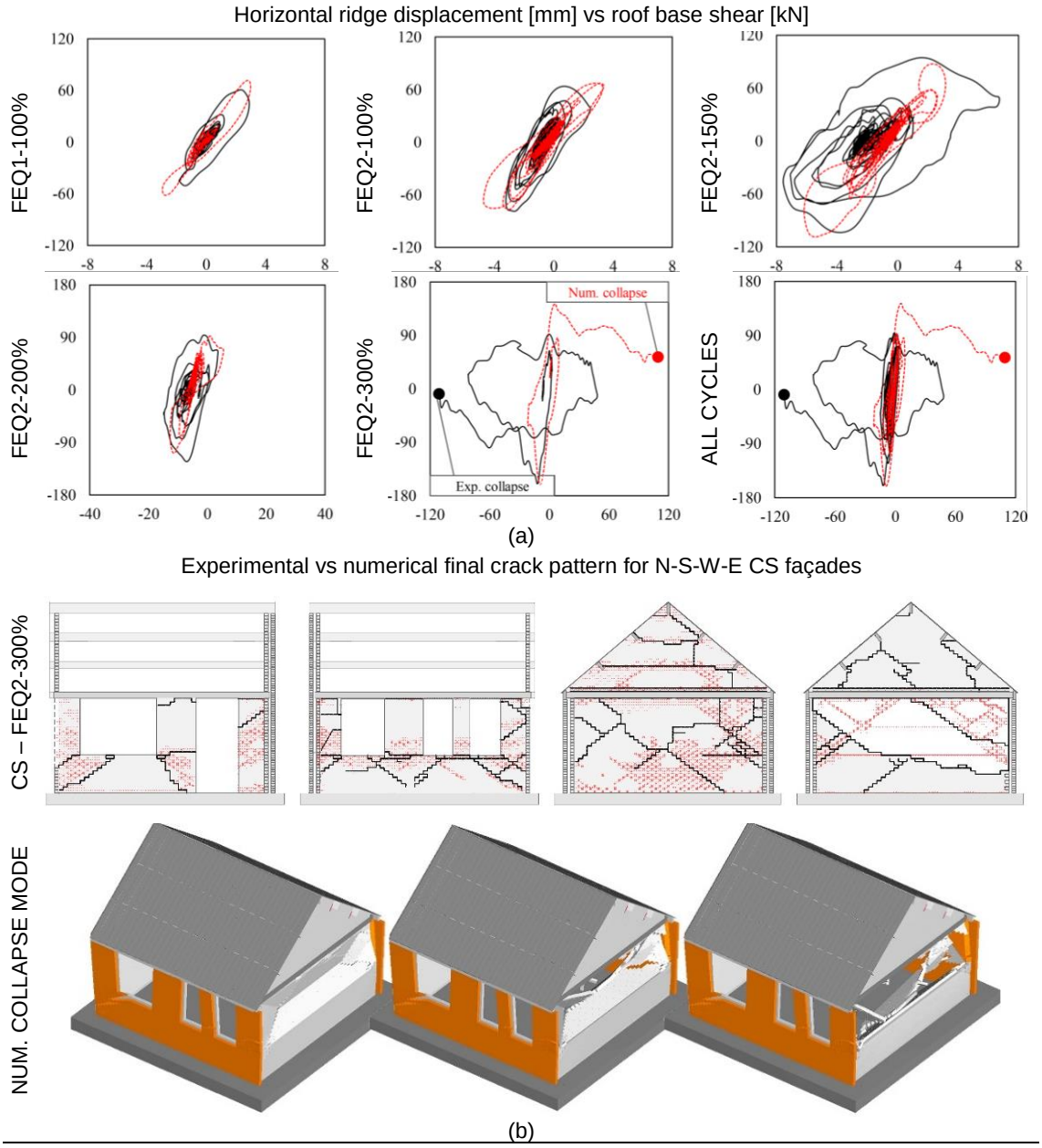

Figure 5. LNEC-BUILD1: Exp. (black line) vs num. (red dashed line) hysteretic response and crack pattern

Simulation of shake-table tests on a complete URM building prototype

The EUC-BUILD1 was tested at the Eucentre laboratory by Graziotti et al. (2017), to which interested readers are referred for further details on experimental layout and loading protocol. Such full-scale building prototype consisted of a two-story cavity-wall system, 5.82 m long, 5.46 m wide and 7.76 m high with a total mass of 56.4 tons, with RC floors, timber roof and construction details analogous to those of LNEC-BUILD1, with the CL veneer not present on one side (see Figure 6) and the slabs only supported by CS transversal walls.

Figure 6. Plan (in cm) and experimental configuration of EUC-BUILD1 (Graziotti et al. 2017)

The specimen was subjected to an incremental dynamic loading sequence, this time up to near-collapse conditions. Both experimental and derived material properties considered for the modelling of EUC-BUILD1 are reported in Table 2 below:

Table 2 Experimental and inferred material properties of EUC-BUILD1

		CS - density δ_m = 1835 [kg/m^3]								CL - density δ_m = 1905 [kg/m^3]							
		fc_m	fc_b	f_w	E_m	c	μ	E_b	E_{mo}	fc_m	fc_b	f_w	E_m	c	μ	E_b	E_{mo}
EUC-BUILD1	Avg [MPa]	6.2	18.7	0.2	4182	0.2	0.4	6628	1574	11.3	45.8	0.2	6033	0.1	0.7	17175	1624
	C.o.V. [%]	0.1	0.1	0.2	0.3	-	-	-	-	0.l	0.03	0.6	0.3	-	-	-	-

From Figure 7(a), where a comparison between test and numerical outcomes is given, it can be gathered that the experimental displacement demand at the different floor levels was satisfactorily represented numerically, as well as the roof deformation.

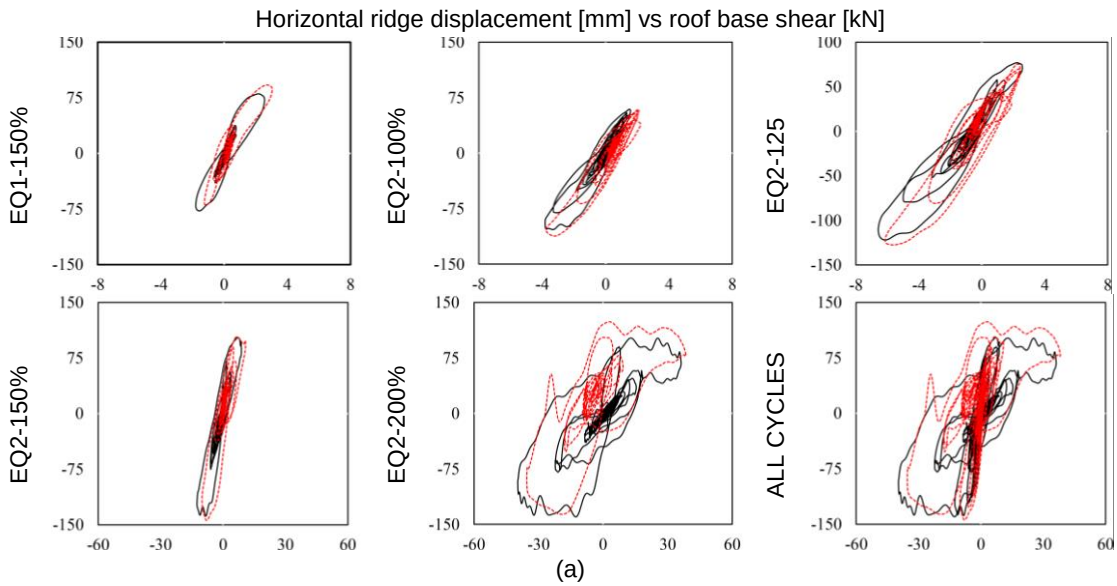

(a)

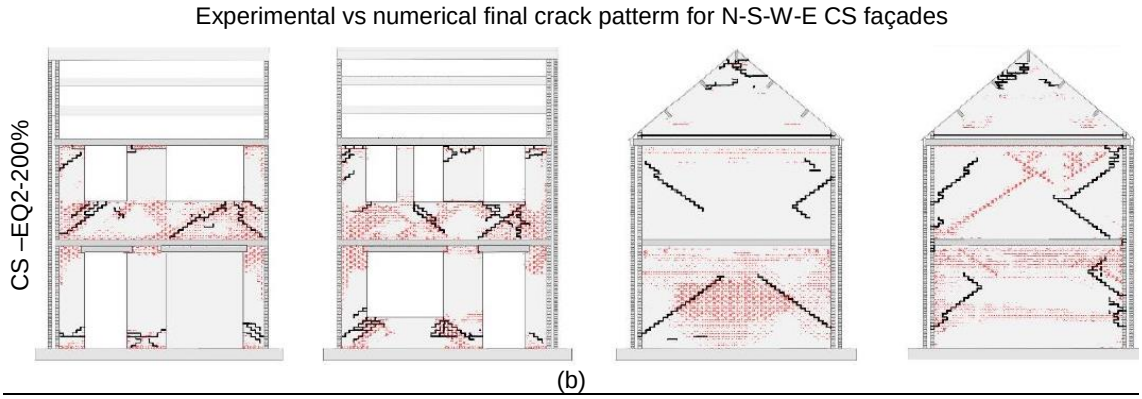

Figure 7. EUC-BUILD1: Exp. (black line) vs num. (red dashed line) hysteretic response and crack pattern

This positive impression is further confirmed by what is shown in Figure 7(b), where experimental and numerical crack propagation patterns appear comparable, albeit the model marginally overestimated the damage in the CS spandrels at EQ2-150% and in the CS transversal façades. Slight differences were also observed in terms of residual roof displacements and overall capacity, especially during EQ2-200%.

Conclusions

In this work, the capability of the Applied Element Method (AEM) to simulate in-plane and out-of-plane mechanisms of URM elements, as well as the behaviour of roof timber systems, were firstly scrutinised and verified through comparison against experimental outcomes on both full-scale components and building sub-structures, up to full collapse. First, the quasi-static cyclic response of a timber roof component was replicated numerically, with a view to calibrate the corresponding AEM model. Then, the shake-table performances of an attic-roof substructure were investigated, up to full collapse, reaching acceptable results both in terms capacity and displacement demand, as well for what concerns the observed OOP collapse mode. Second, a 2nd floor-roof substructure, tested dynamically until up to partial collapse, was considered. Finally, taking advantage of the findings inferred from each of the previous numerical exercises, the modelling of a complete terraced house unit structural system subjected to shake-table testing, was proposed.

Although further improvements are still warranted, perhaps most noteworthy the possibility of including post-peak softening laws in tension for the interface joint model, given that the absence of such modelling capability seems to have led in some cases to an underestimation of the level of dissipated energy, the analyses results seem to indicate that a satisfactorily level of accuracy can indeed be reached with the proposed modelling, given that the predicted hysteretic responses, damage evolutions and collapse modes have shown a good agreement with their experimental counterparts. Further, the experimental displacement demand at the different floor levels was also satisfactorily represented numerically, as was the roof progressive deformation. Thus, given the encouraging results obtained, future developments of the proposed numerical methodology are currently being investigated. Such enhancements might include the extension of the employed methodology to the simulation of more complex large-scale phenomena, such as pounding and dynamic interaction between adjacent terraced house units.

Acknowledgements

The work described in this paper was carried out within the framework of the research programme on hazard and risk of induced seismicity in the Groningen region, sponsored by the Nederlandse Aardolie Maatschappij BV (NAM). The authors also acknowledge all those at both the European Centre for Training and Research in Earthquake Engineering (Eucentre, Pavia, Italy) and Laboratório Nacional de Engenharia Civil (LNEC, Lisbon, Portugal) that were involved in the testing campaign referred to in this paper, and in particular Francesco Graziotti, Umberto Tomassetti and António Correia, for their precious assistance in accessing the test data. Finally, the collaboration of the technical support staff from Applied Science International LLC (ASI), on the use of the employed AEM software - Extreme Loading for Structures, is also acknowledged.

References

Applied Science International LLC. (2018). “Extreme Loading for Structures (2018).” Durham (NC), USA.

Brignola, A., Pampanin, S., and Podestà, S. (2012). “Experimental Evaluation of the In-Plane Stiffness of Timber Diaphragms.” *Earthquake Spectra*, Earthquake Engineering Research Institute, 28(4), 1687–1709.

Brooks, J. J., and Baker, A. (1998). “Modulus of Elasticity of Masonry.” *Masonry International*, 12(2), 58–63.

Calvi, G. M., Moratti, M., O’Reilly, G. J., Scattarreggia, N., Monteiro, R., Malomo, D., Martino Calvi, P., and Pinho, R. (2018). “Once upon a Time in Italy: The Tale of the Morandi Bridge.” *Structural Engineering International*, Taylor & Francis, https://doi.org/10.1080/10168664.2018.1558033.

Chácara, C., Cannizzaro, F., Pantò, B., Caliò, I., and Lourenço, P. B. (2018). “Assessment of the dynamic response of unreinforced masonry structures using a macroelement modeling approach.” *Earthquake Engineering & Structural Dynamics*, John Wiley & Sons, Ltd, 47(12), 2426–2446.

Ciesielski, R. (1999). “The dynamic module of elasticity of brick walls.” *Proceedings of the Conference of the Committee of Civil Engineering PZITB: Lublin, Poland*.

Correia, A. A., Tomassetti, U., Campos Costa, A., Penna, A., Magenes, G., and Graziotti, F. (2018). “Collapse shake-table test on a URM-timber roof substructure.” *16th European Conference on Earthquake Engineering*, Thessaloniki, Greece.

Crowley, H., Pinho, R., van Elk, J., and Uilenreef, J. (2018). “Probabilistic damage assessment of buildings due to induced seismicity.” *Bulletin of Earthquake Engineering*, https://doi.org/10.1007/s10518-018-0462-1.

El-Kashif, K. F., and Maekawa, K. (2004). “Time-dependent nonlinearity of compression softening in concrete.” *Journal of Advanced Concrete Technology*, Japan Concrete Institute, 2(2), 233–247.

van Elk, J., Bourne, S. J., Oates, S. J., Bommer, J. J., Pinho, R., and Crowley, H. (2019). “A Probabilistic Model to Evaluate Options for Mitigating Induced Seismic Risk.” *Earthquake Spectra*, Earthquake Engineering Research Institute, https://doi.org/10.1193/050918EQS118M.

Galvez, F., Giaretton, M., Abeling, S., Ingham, J., and Dizhur, D. (2018). “Discrete Element modelling of a two-storey unreinforced masonry scaled model.” *16th European Conference on Earthquake Engineering*, Thessaloniki, Greece.

Gattesco, N., and Macorini, L. (2014). “In-plane stiffening techniques with nail plates or CFRP strips for timber floors in historical masonry buildings.” *Construction and Building Materials*, Elsevier, 58, 64–76.

Graziotti, F., Penna, A., and Magenes, G. (2018). “A comprehensive in situ and laboratory testing programme supporting seismic risk analysis of URM buildings subjected to induced earthquakes.” *Bulletin of Earthquake Engineering*, Springer Netherlands, https://doi.org/10.1007/s10518-018-0478-6.

Graziotti, F., Tomassetti, U., Kallioras, S., Penna, A., and Magenes, G. (2017). “Shaking table test on a full scale URM cavity wall building.” *Bulletin of Earthquake Engineering*, Springer Netherlands, 15(12), 5329–5364.

Grunwald, C., Khalil, A. A., Schaufelberger, B., Ricciardi, E. M., Pellecchia, C., De Iuliis, E., and Riedel, W. (2018). “Reliability of collapse simulation – Comparing finite and applied element method at different levels.” *Engineering Structures*, Elsevier, 176, 265–278.

Jäger, W., Irmschler, H., and Schubert, P. (2004). *Mauerwerk-Kalender 2004*. Ernst & Sohn Verlag für Architektur und technische Wissenschaften.

Kallioras, S., Graziotti, F., and Penna, A. (2019). “Numerical assessment of the dynamic response of a URM terraced house exposed to induced seismicity.” *Bulletin of Earthquake Engineering*, 17(3), 1521–1552.

Karbassi, A., and Nollet, M.-J. (2013). “Performance-based seismic vulnerability evaluation of masonry buildings using applied element method in a nonlinear dynamic-based analytical procedure.” *Earthquake Spectra*, Earthquake Engineering Research Institute, 29(2), 399–426.

Kaushik, H. B., Rai, D. C., and Jain, S. K. (2007). “Stress-strain characteristics of clay brick masonry under uniaxial compression.” *Journal of materials in Civil Engineering*, American Society of Civil Engineers, 19(9), 728–739.

Malomo, D. (2019). “Discrete Element models for the seismic assessment of unreinforced masonry structures.” *PhD Thesis, University of Pavia, Italy*.

Malomo, D., Comini, P., Pinho, R., and Penna, A. (2018a). “The Applied Element Method and the modelling of both in-plane and out-of-plane response of URM walls.” *16th European Conference on Earthquake Engineering*, Thessaloniki, Greece.

Malomo, D., DeJong, M. J., and Penna, A. (2019). “Distinct Element modelling of the in-plane cyclic response of URM piers subjected to shear-compression.” *Earthquake Engineering & Sructural Dynamics - in press*.

Malomo, D., Pinho, R., and Penna, A. (2018b). “Using the Applied Element Method to simulate the dynamic response of full-scale URM houses tested to collapse or near-collapse conditions.” *16th European Conference on Earthquake Engineering*, Thessaloniki, Greece.

Malomo, D., Pinho, R., and Penna, A. (2018c). “Using the applied element method for modelling calcium silicate brick masonry subjected to in-plane cyclic loading.” *Earthquake Engineering & Structural Dynamics*, 47(7), 1610–1630.

Matysek, P., and Janowski, Z. (1996). “Analysis of factors affecting the modulus of elasticity of the walls.” *Proceedings of the Conference of the Committee of Civil Engineering PZITB: Lublin, Poland*.

Meguro, K., and Tagel-Din, H. (2000). “Applied element method for structural analysis: Theory and application for linear materials.” *Structural Engineering/Earthquake Engineering*, Japan Society of Civil Engineers, 17(1), 21s--35s.

Meguro, K., and Tagel-Din, H. (2001). “Applied Element Simulation of RC Structures under Cyclic Loading.” *Journal of Structural Engineering*, 127(11), 1295–1305.

Meguro, K., and Tagel-Din, H. (2002). “Applied Element Method Used for Large Displacement Structural Analysis.” *Journal of Natural Disaster Science*, 24(1), 25–34.

Messali, F., Esposito, R., and Maragna, M. (2016). “Pull-out strength of wall ties.” *Report, TU Delft, NL*.

Salem, H., Mohssen, S., Kosa, K., and Hosoda, A. (2014). “Collapse Analysis of Utatsu Ohashi Bridge Damaged by Tohuku Tsunami using Applied Element Method.” *Journal of Advanced Concrete Technology*, Japan Concrete Institute, 12(10), 388–402.

Tomassetti, U., Correia, A. A., Candeias, P. X., Graziotti, F., and Campos Costa, A. (2018). “Two-way bending out-of-plane collapse of a full-scale URM building tested on a shake table.” *Bulletin of Earthquake Engineering*, Springer Netherlands, 17(4), 2165–2198.

U.B.C. (1991). “International Conference of Building Officials. Uniform Building Code.” *International conference of building officials, USA*, Whittier, USA.